The PDZ-interacting domain of TRPC4 controls its localization and surface expression in HEK293 cells

Laurence Mery[1,*], Bettina Strauß[1], Jean F. Dufour[2], Karl H. Krause[3] and Markus Hoth[1]

[1]Department of Physiology, University of Saarland, D-66421 Homburg, Germany
[2]Department of Clinical Pharmacology, University of Bern, Murtenstrasse 35, 3010 Bern, Switzerland
[3]Department of Geriatrics, Geneva University Hospital, CH-1211 Geneva 14, Switzerland
*Author for correspondence (e-mail: phlmery@uniklinik-saarland.de)

Accepted 14 June 2002
Journal of Cell Science 115, 3497-3508 © 2002 The Company of Biologists Ltd

Summary

Mammalian homologs of the *Drosophila* TRP protein have been shown to form cation-permeable channels in the plasma membrane but very little is known about the mechanisms that control their cell surface localization. Recently it has been demonstrated that the last three C-terminal amino acids (TRL) of TRPC4 comprise a PDZ-interacting domain that binds to the scaffold protein EBP50 [ezrin/moesin/radixin-binding phosphoprotein 50]. In this report, we have examined the influence of the TRL motif on the subcellular distribution of TRPC4 in human embryonic kidney (HEK) 293 cells. We have also analyzed the consequences of the interaction between EBP50 and the membrane-cytoskeletal adaptors of the ezrin/radixin/moesin (ERM) family for the cell surface expression of TRPC4. Using immunofluorescence microscopy, we found that the mutant lacking the TRL motif accumulated into cell outgrowths and exhibited a punctate distribution pattern whereas the wild-type channel was evenly distributed on the cell surface. Deletion of the PDZ-interacting domain also decreased the expression of TRPC4 in the plasma membrane by 2.4-fold, as assessed by cell surface biotinylation experiments. Finally, in a large percentage of cells co-expressing TRPC4 and an EBP50 mutant lacking the ERM-binding site, TRPC4 was not present in the plasma membrane but co-localized with the truncated scaffold in a perinuclear compartment (most probably representing the Golgi apparatus) and in vesicles associated with actin filaments. Our data demonstrate that the PDZ-interacting domain of TRPC4 controls its localization and surface expression in transfected HEK293 cells. They also point to a yet unexplored role of the EBP50-ERM complex in the regulation of protein insertion into the plasma membrane.

Key words: TRPC proteins, PDZ domain, EBP50, Membrane localization

Introduction

The expression of an ion channel at the cell surface depends on a program of events that includes transcription of the genes encoding the channel components, insertion of the nascent polypeptides into the endoplasmic reticulum membrane, subunit oligomerization and routing of the assembled channel to the plasma membrane. Transcription is a highly regulated step and numerous factors (including developmental stage and hormones) have been shown to modulate channel message levels and consequently plasma membrane conductances. However, recent work indicates that protein processing also plays a key role in the control of channel number and activity at the cell surface.

Over the last years, the cDNAs encoding a large number of ion channels have been cloned and, in parallel, mutations that affect channel properties have been identified. It has become obvious that in a number of 'channelopathies', the defect is associated with a failure of the intracellular sorting machinery to deliver an otherwise functional channel to its correct destination. This is true for the CFTR mutation ΔF^{508}, which occurs in nearly 70% of cystic fibrosis patients among Caucasians (Cheng et al., 1990; Pasyk and Foskett, 1997), as well as for HERG potassium channel mutations that cause the cardiac 'long Q-T' syndrome (Zhou et al., 1998). Other diseases (such as Liddle's syndrome) are caused by a gain of channel function due to an increased stability of the channel at the plasma membrane (Rotin et al., 2001). These findings have prompted a number of groups to look for specific signals within the amino acid sequence of channel proteins that could regulate their intracellular transport and surface localization. By using domain swap or deletion experiments as well as site-directed mutagenesis, several types of motifs have been identified including the PDZ-binding domains. The latter correspond to short consensus sequences (S/T-X-L/V/I/M or F/Y-X-F/Y/A, where X is any amino acid) located at the C-terminus of numerous receptors, ion channels and transporters (Songyang et al., 1997). PDZ-binding domains specifically interact with modular 80-90 amino acid sequences named PDZ domains after PDS-95, Dlg-A and ZO-1, three proteins in which these motifs were first described.

A clear demonstration for a role of a PDZ domain protein in channel localization has emerged from analysis of *Drosophila* phototransduction. Vision in *Drosophila* uses the fastest known PLC-dependent signaling cascade, taking just a few milliseconds to go from activation of rhodopsin to the generation of a receptor potential and less than 100 milliseconds to terminate the response (for a review, see Montell, 1999). An important strategy used by *Drosophila*

photoreceptors to both increase vision speed and allow a fine tuning of the light response, is the organization of the signaling components into a macromolecular complex (or transducisome) via the adaptor protein INAD (inactivation no afterpotential D). INAD (Shieh and Niemeyer, 1995) consists primarily of five PDZ domains and can bind directly to different proteins (Montell, 1999) including protein kinase C (PKC), phospholipase C (PLC), the light-activated cation channel TRP and the actin-binding protein NINAC. The transducisomes localize to the rhabdomeres, a subcellular compartment consisting of 60,000 microvilli and containing the 10^8 molecules of rhodopsin found in *Drosophila* photoreceptors. In *inaD* null mutants, photoreceptors have profound signaling defects (Chevesich et al., 1997; Tsunoda et al., 1997). TRP, PLC and PKC no longer localize to the rhabdomeres, but instead are randomly distributed throughout either the plasma membrane (in the case of TRP) or the cytoplasm (PLC and PKC). Recent studies have shown that the INAD-TRP interaction is not required for targeting but rather for anchoring of the preassembled transducisomes in the rhabdomere (Li and Montell, 2000; Tsunoda et al., 2001).

While it is accepted that members of the TRPC subfamily of *Drosophila* TRP homologs form channels that are activated in a PLC-dependent manner (Clapham et al., 2001), the mechanisms that control their assembly and cell surface expression are largely unknown. It has recently been suggested that the PDZ domain protein NHERF (Na^+/H^+ exchanger regulatory factor) (Weinman et al., 1995) and its human ortholog EBP50 [ezrin/radixin/moesin (ERM)-binding phosphoprotein 50] (Reczek et al., 1997) may be functional analogs of INAD in mammalian cells. Indeed, the PDZ domains of NHERF have been shown to bind to several members of the phospholipase Cβ family (Reczek and Bretscher, 2001; Tang et al., 2000) and to the mammalian TRP homologs TRPC4 and TRPC5 (Tang et al., 2000). In addition, NHERF interacts with the actin-binding proteins of the ERM family (Reczek et al., 1997) via its C-terminal 30 amino acids and may link the PLC-β and TRPC4/5 to the cytoskeleton. In this study, we demonstrate that the PDZ-binding domain of TRPC4 controls its localization and surface expression in transfected human embryonic kidney (HEK) 293 cells. Our results also suggest that the interaction between EBP50 and the membrane-cytoskeletal adaptors of the ERM family may play an active role in the cell surface delivery of TRPC4 by facilitating the translocation of TRPC4-bearing vesicles from the cortical actin layer to the plasma membrane.

Materials and Methods

Materials

DMEM-F12, fetal calf serum, penicillin/streptomycin and trypsin were purchased from Life Technologies. Chemical reagents were obtained from Sigma. Glutathione-sepharose 4B and the Enhanced Chemiluminescence (ECL) detection system were purchased from Amersham Pharmacia Biotech. EZ-link™ Sulfo-NHS-LC-biotin and Immuno-pure immobilized avidin were obtained from Pierce. JEG-3 cells and human embryonic kidney (HEK) 293 cells were from the American Type Culture Collection (Rockville, MD). Oligonucleotides were synthesized by Life Technologies and restriction enzymes were purchased from Eurogentec. The anti-YFP and anti-myc monoclonal antibodies were obtained from Boehringer Mannheim. The anti-ezrin antibody was purchased from Biogenesis (Poole, UK). The anti-CD4, anti-vimentin and anti β-tubulin monoclonal antibodies were from Sigma. The polyclonal anti-NHERF antibody (which also recognizes EBP50) was a generous gift from E. J. Weinman (Department of Medicine and Physiology, University of Maryland School of Medicine, Baltimore, MD).

Plasmid constructions

PolyA$^+$ mRNA was purified from HEK293 cells using the Fast Track 2.0 kit (InVitrogen, Groningen, The Netherlands). First strand cDNA was synthesized by using the AMV reverse transcriptase (InVitrogen) and oligo-dT as primers. The entire coding region of the EBP50 cDNA was then amplified by PCR. The resulting product was gel purified, subcloned into the pGEM-T vector (Promega) and sequenced (MWG biotech). The cDNA sequences encoding residues 10-101 and 144-247 of EBP50 were amplified by PCR using mutant primers containing appropriated restriction sites. The resulting products, encoding either the PDZ1 or the PDZ2 domain of EBP50, were then subcloned into the pGEX-5X-1 vector (Amersham Pharmacia biotech) to produce glutathione-S-transferase (GST)-PDZ fusion proteins.

The cDNA encoding YFP-EBP50 was generated as follows: the coding region of EBP50 was amplified by PCR. A *Bgl*II site was introduced at the 3′end, after the stop codon, to facilitate subsequent cloning. The start codon (ATG) was replaced by the GCT nucleotides to create a *Nhe*I site (5′-GCTAGC-3′). The region corresponding to nucleotides 1879-2621 of the pIRES-EYFP vector (Clontech), encoding the enhanced yellow fluorescent protein (EYFP), was amplified by PCR. In the antisense primer, the stop codon (TAA) was replaced by a TCT codon. The latter was included into a *Xba*1 site (5′-TCTAGA-3′) to allow the fusion in frame with EBP50. The resulting products were gel purified and ligated into pGEM-T [leading to the pGEM/EBP50(ΔMet) and pGEM/EYFP(Δstop) constructs]. All recombinant sequences were determined to be free of PCR errors by nucleotide sequence analysis. The *Nhe*I-*Sac*I fragment was excised from pGEM/EBP50(ΔMet) and subcloned into the *Xba*I-*Sac*I sites of pGEM/EYFP(Δstop). The resulting construct was then digested with *Bam*HI and *Not*I and inserted into pcDNA$_3$(+) (InVitrogen). The EBP50 mutant lacking the ERM-binding domain was generated as follows: the region corresponding to nucleotides 596-1193 of the EBP50 cDNA was amplified by PCR using pGEM/EBP50 as template. Nucleotides 1191-1193 (which encodes A^{328}) were replaced by the TAG stop codon using a sequence-mutated antisense primer. The PCR product was subcloned into the pGEM-T vector. Following sequence analysis, the insert was excised from pGEM using *Eco*RI and *Not*I and ligated into pcDNA$_3$/YFP-EBP50. The resulting construct encodes a YFP-EBP50 fusion protein lacking the 31 EBP50 C-terminal amino acids and referred to as YFP-ΔERM. Nucleotides are numbered according to the sequence deposited in the GenBank under the accession number AF015926.

The cDNA encoding TRPC4 (accession number AAF22928) was isolated as previously described and subcloned into the pGEM-T vector. The 5′ untranslated region was removed and the construct was epitope-tagged at the N-terminus with the myc peptide MEQKLISEEDLLR. The first methionine codon was included within the sequence characteristic for translation initiation 5′-GCCGCCATGG-3′ as specified previously (Kozak, 1991). The TRPC4 mutant lacking the last three C-terminal amino acids (called myc-ΔTRL) was generated by PCR-based mutagenesis. The region corresponding to nucleotides 2644-2907 of the TRPC4 cDNA was amplified and the nucleotides 2905-2907 encoding T^{890} were replaced by a premature stop codon in the antisense primer. The resulting product was inserted into pGEM-T. Sequencing was performed to confirm the deletion and to verify that base misincorporation did not occur during DNA amplification. The PCR fragment was then excised from pGEM using *Xho*I and *Not*I and ligated into the similarly cut pGEM/myc-TRPC4. The cDNAs encoding myc-TRPC4 and myc-

ΔTRL were then subcloned into the *Not*I site of pcDNA$_3$(+) (InVitrogen). All PCR primers sequences are available upon request.

Cell culture and transfection

HEK293 cells and JEG-3 cells were cultured in DMEM-F12 medium supplemented with 10% heat-inactivated fetal calf serum, 50 U/ml penicillin and 50 μg/ml streptomycin. Transfections were carried out by the calcium phosphate co-precipitation method as previously described (Mery et al., 2001).

GST-pulldown assays

GST-PDZ1, GST-PDZ2 as well as the GST alone were expressed in BL21 *E. coli* strain. Production of the fusion proteins was initiated by adding 0.1 mM isopropyl-β-thio-D-galactopyranoside (IPTG) to the bacterial cultures grown to an A_{600} of 0.6. After 90 minutes of induction at 37°C, bacteria were harvested and resuspended in ice-cold PBS containing 1% Triton X-100, 1 mM EDTA and a cocktail of protease inhibitors (Boehringer Mannheim). Bacteria were lysed by three cycles of rapid freeze/thawing followed by 12 passages through a 23-gauge needle. The insoluble material was removed by centrifugation for 5 minutes at 10,000 ***g*** and 4°C and the supernatant was incubated with glutathione-sepharose beads for 1 hour at room temperature. After four washes with the lysis buffer, an aliquot of beads was removed: bound proteins were released by incubating the beads in 2× Laemmli buffer (125 mM Tris-HCl, 20% glycerol, 6% SDS, 10% β-mercaptoethanol, pH 6.8) for 15 minutes at 37°C. Eluates were analyzed on 12% SDS-PAGE and then stained with Coomassie blue. HEK293 cells expressing either myc-TRPC4 or myc-ΔTRL as well as the mock-transfected cells were lysed 48 hours after transfection in PBS containing 1% Triton X-100, 1 mM EDTA and a cocktail of protease inhibitors (Boehringer Mannheim). Protein concentrations were determined with the bicinchonic acid (BCA) procedure (Sigma) using bovine serum albumin as standard. Samples (200 μg of triton-solubilized proteins) were incubated for 3 hours at 4°C with glutathione-sepharose beads, charged with either GST, GST-PDZ1 or GST-PDZ2. The beads were then harvested by centrifugation and washed four times with the lysis buffer at 4°C. Bound proteins were eluted with 50 μl of 2× Laemmli buffer and analyzed, together with aliquots of the total cell extracts, by SDS-PAGE and immunoblot.

Co-immunoprecipitation

48 hours after transfection, HEK293 cells were rinsed twice with PBS pH 7.4 and then collected from plates without trypsinisation, by incubation in the same buffer supplemented with 2 mM EDTA. The harvested cells were centrifuged at 1000 ***g*** and 4°C for 5 minutes and resuspended in ice-cold lysis buffer (PBS pH 7.4 containing 1% triton, 1 mM EDTA and a cocktail of protease inhibitors). The lysates were rotated at 4°C for 30 minutes to further solubilize the proteins and cellular debris were removed by centrifugation for 5 minutes at 1000 ***g*** and 4°C. Samples (300 μg of proteins) were mixed with anti-YFP antibodies (2 μg) and rotated for 90 minutes at 4°C. Antigen-antibody complexes were then precipitated by adding 50 μl of protein G-agarose beads (Roche diagnostics) pre-equilibrated in the lysis buffer. After rocking the reaction mixtures for 16 hours at 4°C, the beads were pelleted and washed four times with the lysis buffer. The immunoprecipitates were eluted by boiling the samples in 50 μl 2× Laemmli buffer for 5 minutes and then fractionated by SDS-PAGE.

Cell surface biotinylation

Dishes with confluent transfected HEK293 cells were placed on ice and washed twice with ice-cold PBS pH 8 containing 1 mM $MgCl_2$ and 0.5 mM $CaCl_2$ (PBSB). Cells were then incubated for 30 minutes at 4°C with NHS-LC-biotin (final concentration 0.5 mg/ml), freshly diluted in PBSB. Biotinylation was terminated by rinsing the dishes twice with PBSB containing 0.1% bovine serum albumin (to quench the unbound NHS-LC-biotin) and once with PBS pH 7.4 without Ca^{2+}/Mg^{2+}. Cells were collected from plates without trypsinisation and lysed as described above. Following measurement of the protein content of the cell extract, samples (900 μg of protein) were added to 200 μl of avidin-agarose beads, pre-equilibrated in the lysis buffer and rotated for 3 hours at 4°C. The biotin-avidin agarose complexes were then harvested by centrifugation and washed four times with the lysis buffer supplemented with 0.25 M NaCl (final concentration 0.4 M NaCl). The beads were then resuspended in 150 μl of 2× Laemmli buffer and incubated at 37°C for 15 minutes prior to SDS-PAGE. Experiments were carried out to rule out that: (1) cytosolic proteins in damaged cells are biotinylated and thus contribute to the pool assumed to represent surface molecules; and (2) intracellular myc-tagged proteins can bind to avidin-agarose beads in a biotin-independent way. As shown in Fig. 5C, YFP was found in the lysate from the biotinylated HEK293 monolayers but not in the fraction recovered from the avidin beads. Similarly, myc-tagged channels were not detected in affinity precipitates from myc-TRPC4- or myc-ΔTRL-expressing cells not exposed to NHS-LC-biotin.

Preparation of membrane fractions

Transfected HEK293 cells were grown to confluence, washed with PBS pH 7.4 and then collected from plates without trypsinisation, by incubation in PBS containing 2 mM EDTA for 2 minutes. The cells were centrifuged at 700 ***g*** for 5 minutes, resuspended in ice-cold lysis buffer (50 mM Tris-HCl buffer pH 7.5 supplemented with 10 mM KCl, 1.5 mM $MgCl_2$, 1 mM EDTA and protease inhibitors) and rotated at 4°C for 30 minutes. The cells were subjected to three freeze-thaw cycles and then sheared 10 times with 23-gauge needles. Normal osmolarity was restored by adding 150 mM NaCl. Postnuclear supernatants, prepared by spinning the cell homogenate at 1000 ***g*** and 4°C for 10 minutes, were then centrifuged for 1 hour at 100,000 ***g*** and 4°C in a TI60 rotor (Beckman Coulter), resulting in a clear cytoplasmic fraction and a membrane pellet. The latter was washed once with the lysis buffer supplemented with 150 mM NaCl and then solubilized in PBS containing 1% triton, 0.2% SDS and a cocktail of protease inhibitors at 4°C. The insoluble material was removed by centrifugation at 10,000 ***g*** for 5 minutes at 4°C. Protein concentrations were determined with the bicinchonic acid procedure (Sigma) using bovine serum albumin as standard. Isolated crude membranes were subjected to SDS-PAGE.

SDS-PAGE and immunoblots

Proteins were fractionated on a SDS-PAGE polyacrylamide gel and electrophoretically transferred to Immobilon-P membranes (Millipore Corp.) in 25 mM Tris-HCl, 0.19 M glycine and 20% ethanol. The polyvinylidene difluoride membranes were blocked overnight at 4°C in PBS containing 5% nonfat dry milk and 0.05% Tween-20, rinsed twice with water and then incubated for 2 hours at room temperature with the primary antibody (anti-myc or anti-YFP) diluted 1:1000 in PBS supplemented with 0.05% Tween-20 and 2.5% nonfat milk. After three washes with PBS/0.05% Tween-20, the membranes were allowed to react for 1 hour at room temperature with a peroxidase-conjugated goat anti-mouse IgG antibody, diluted 1:10,000 in PBS/0.05% Tween-20. The blots were washed three times with PBS/0.05% Tween-20 and the immune complexes were visualized by chemiluminescence. When required, bands were quantified with a LKB Ultrascan XL laser densitometer and the ImageQuant software.

Indirect immunofluorescent microscopy

HEK293 and JEG-3 cells were seeded on polyornithine-coated

coverslips at low density. Twenty-four hours after the plating, HEK293 cells were co-transfected with 0.9 μg of the vector encoding either myc-TRPC4 or the ΔTRL mutant and 0.3 μg of the plasmid encoding YFP-EBP50. JEG-3 cells were transfected with 0.5 μg of the vector encoding either the YFP alone, YFP-EBP50 or YFP-ΔERM. Two days after the transfection, cells were rinsed twice with PBS pH 7.4 containing 1 mM $CaCl_2$ and 0.5 mM $MgCl_2$ (PBS C/M), fixed in 4% paraformaldehyde for 15 minutes and then permeabilized using 0.4% triton for 3 minutes. Blocking of nonspecific binding sites was performed by incubating the monolayers with PBS-C/M containing 0.2% gelatin and 2% normal goat serum (Sigma) for 30 minutes. Transfected cells were stained for 1 hour with the primary antibody at the indicated dilutions [anti-CD4 (1:200), anti-myc (1:300), anti-NHERF/EBP50 (1:200), anti-ezrin (1:200), anti-β-tubulin (1:200), anti-vimentin (1:100), rhodamine-phalloidin (1:200)], washed three times with the blocking solution and then incubated for 1 hour with a 1:300 dilution of the appropriate secondary antibody [Alexa 594-conjugated anti-mouse IgG or Alexa 488-conjugated anti-rabbit IgG (Molecular probes)]. All antibody dilutions were prepared in PBS-C/M supplemented with 0.2% gelatin and 2% normal goat serum and the incubations were carried out at room temperature. After extensive washing with PBS-C/M, coverslips were mounted using Prolong antifade reagent (Molecular Probes) and viewed with an upright Olympus BX50 fluorescence microscope equipped with a 75W Xe arc lamp and with standard FITC and Texas Red filter sets (AHF Analysentechnik, Germany). Images were collected through an Olympus 100× oil immersion objective (UPlanApo, NA 1.35) with a CCD camera (Sony) and digitized with microslicer imaging software (Bernd Lindemann, Homburg). For some experiments, adherent cells were pre-extracted in buffer A (140 mM KCl, 10 mM NaCl, 2 mM $MgCl_2$, 10 mM Hepes, 0.1 mM $CaCl_2$, 1.1 mM EGTA pH 7.2) containing 10 μg/ml digitonin for 5 minutes on ice before fixation with 4% PFA in buffer A. The fixed cells were washed twice with buffer A, twice with PBS C/M and then processed as previously described.

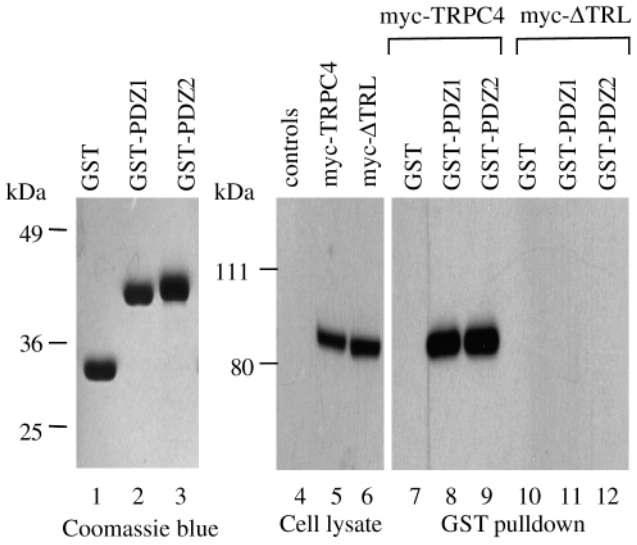

Fig. 1. TRPC4 associates with both PDZ domains of EBP50 through its C-terminal TRL motif. Triton extracts of HEK293 cells expressing either myc-TRPC4 or myc-ΔTRL were incubated for 3 hours at 4°C with glutathione-sepharose beads loaded with either GST, GST-PDZ1 or GST-PDZ2. After extensive washing, bound proteins were analyzed by SDS-PAGE, transferred to PVDF and probed with an anti-myc antibody (right panel). The middle panel demonstrates that myc-TRPC4 and myc-ΔTRL were expressed at comparable levels in the transfected cells. Note that control cells (lane 4) transfected with the empty vector failed to react with the anti-myc antibody, implying that the immunoreactivity is specific for the myc epitope. The left panel shows the amount of GST or GST-fusion proteins used, as revealed by Coomassie Blue staining. Lanes 4-6 contain 10% of the extract used for the binding assay and lanes 7-12 contain 40% of the eluate. Results shown are representative of three independent experiments.

Results

Removal of the TRL motif at the C-terminus of TRPC4 abolishes the interaction with both PDZ domains of EBP50

Given that a number of studies have demonstrated the importance of PDZ-domain-containing proteins in ion channel trafficking, we set out to investigate how EBP50 influences TRPC4 localization and surface delivery in HEK293 cells. A mutant lacking the PDZ-interacting consensus formed by the last three C-terminal amino acids (TRL^{893}) of TRPC4 was generated. A myc tag was added at the N-terminus of both wild-type and truncated TRPC4 molecules to facilitate detection and the resulting constructs were referred to as myc-TRPC4 and myc-ΔTRL, respectively. To test whether the deletion of the TRL motif at the C-terminus of TRPC4 is sufficient to abolish the interaction with EBP50, we performed GST-pulldown experiments. Both PDZ domains of EBP50 were expressed as GST fusion proteins and purified by immobilization on glutathione-sepharose beads. The immobilized proteins were then incubated with lysates from HEK293 cells expressing either myc-TRPC4 or myc-ΔTRL. After extensive washing, bound proteins were eluted and analyzed, together with aliquots of total cell extracts, by immunoblotting. As shown in Fig. 1, GST-PDZ1 (lane 8) and GST-PDZ2 (lane 9) were found to retain myc-TRPC4 equally well, whereas no interaction was seen between myc-TRPC4 and the GST alone (lane 7). In contrast to myc-TRPC4, myc-ΔTRL was not detected in any of the precipitates (Fig. 1, lanes 10-12), demonstrating that the C-terminal end of TRPC4 is required for the interaction with EBP50.

Addition of a YFP tag at the N-terminus of EBP50 facilitates its detection without affecting its subcellular localization

To be able to study the localization of the scaffold protein in both living and fixed cells, we generated a cDNA construct encoding EBP50 N-terminally fused to the yellow fluorescent protein (YFP). In JEG-3 cells, which derive from placental syncytiotrophoblasts, EBP50 is particularly abundant and specifically associates with the numerous microvilli of the apical surface. To rule out the possibility that addition of the YFP tag affects EBP50 localization or trafficking, the fusion protein was expressed in JEG-3 cells and its subcellular distribution was analyzed by indirect immunofluorescence microscopy. As shown in Fig. 2, the staining pattern of YFP-EBP50 (Fig. 2C) was very similar to that seen for ezrin (Fig. 2A) or endogenous EBP50 (Fig. 2B). In contrast, the YFP (Fig. 2D) was mainly found in the cytosol and the nucleus of transfected cells.

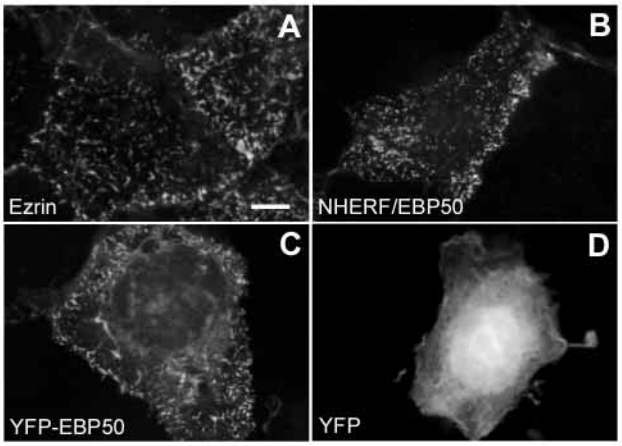

Fig. 2. Subcellular distribution of YFP-EBP50 in human JEG-3 cells. (A,B) Human JEG-3 cells, grown on coverslips, were fixed with PFA, permeabilized with triton and probed with antibodies directed against either ezrin (A) or NHERF/EBP50 (B). The cells were then stained with a secondary antibody conjugated to either Alexa 594 (A) or Alexa 488 (B). (C,D) JEG-3 cells transiently expressing YFP-EBP50 (C) or the YFP alone (D) fixed with PFA. Images were acquired with a 100× oil immersion objective and filter sets for Texas Red (A) and FITC (B-D). Bar, 20 μm.

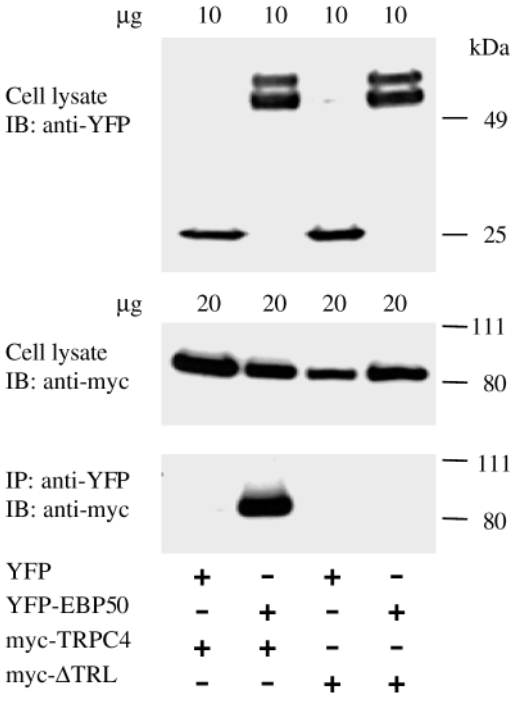

Fig. 3. YFP-tagged EBP50 co-immunoprecipitates with myc-TRPC4 but not with the mutant lacking the last three C-terminal residues. myc-TRPC4 or myc-ΔTRL were transiently expressed in HEK293 cells together with YFP alone or YFP-EBP50. Detergent extracts of the transfected cells were incubated with an anti-YFP antibody and protein G-coated agarose beads. 40% of the precipitated proteins were separated by SDS-PAGE, transferred to PVDF and immunoblotted with an anti-myc antibody (lower panel). Middle panel: cell lysates (17% of the input used for the co-immunoprecipitation) probed with anti-myc antibody to detect myc-TRPC4 and myc-ΔTRL Upper panel: cell lysates probed with anti-YFP antibody to detect YFP and YFP-EBP50. Size markers indicate the molecular mass in kDa. IB, immunoblot; IP, immunoprecipitation. Results shown are representative of three independent experiments.

Deletion of the TRL motif prevents the association of TRPC4 with YFP-EBP50 in HEK293 cells

To determine whether YFP-EBP50 can bind to TRPC4 in a cellular context, co-immunoprecipitation experiments were performed. YFP-EBP50 or YFP were co-expressed with either myc-TRPC4 or myc-ΔTRL in HEK293 cells. As shown in Fig. 3 (lower panel), myc-TRPC4 can be co-immunoprecipated with YFP-EBP50 but not with the YFP alone. Removal of the TRL motif completely abolished the association with the scaffold protein, indicating that formation of the TRPC4/YFP-EBP50 complex in HEK293 cells requires the PDZ-binding cassette of TRPC4. Note that expression of YFP-EBP50 in HEK293 cells allowed immunological detection of two bands at 65-70 kDa with antibodies to YFP (Fig. 3, top panel). Treatment of the cell lysate with calf intestinal phosphatase resulted in the collapse of the 70 kDa band into the 65 kDa species (data not shown), indicating that the heterogeneity was due to phosphorylation. Thus, YFP-EBP50, similar to endogenous EBP50, is constitutively phosphorylated in HEK293 cells, possibly by the G protein-coupled receptor kinase 6A (GRK6A) (Hall et al., 1999).

Deletion of the TRL motif dramatically alters the subcellular distribution of TRPC4 in HEK293 cells

Indirect immunofluorescence microscopy was then used to analyze the distribution of myc-TRPC4 and myc-ΔTRL in HEK293 cells co-expressing YFP-EBP50. The localization of the myc-tagged molecules was compared with that of CD4, a transmembrane protein that does not interact with EBP50. In agreement with the idea that the N-terminal domain of TRP proteins is oriented towards the cytoplasm, myc-TRPC4 and myc-ΔTRL were detected in cells permeabilized with either Triton X-100 (Fig. 4J,L) or digitonin (Fig. 4P,R) but not in intact cells (Fig. 4D,F). As shown in Fig. 4B, non permeabilized CD4-expressing cells were heavily stained with an antibody directed against the extracellular domain of the receptor, indicating that CD4 was highly expressed on the surface membrane. In triton-permeabilized cells, the staining patterns of CD4 (Fig. 4H) and myc-TRPC4 (Fig. 4J) looked very similar. Both proteins were found to be evenly distributed at the plasma membrane and to localize to a juxtanuclear compartment, most probably representing the Golgi apparatus. In contrast, the mutant lacking the TRL motif accumulated into cell outgrowths and exhibited a clustered appearance (Fig. 4L). The latter was very similar to the patchy staining that has been described for murine TRPC4 C-terminally fused to the GFP and expressed in HEK293 cells (Schaefer et al., 2000). These findings suggest that EBP50 or another PDZ protein with similar specificity [such as the NHE3-kinase A regulatory protein (E3KARP) (Yun et al., 1997), the CFTR-associated protein 70 (CAP70) (Wang et al., 2000), or the CFTR-associated ligand (CAL) (Cheng et al., 2001)] controls TRPC4 localization in HEK293 cells.

Expression of YFP-EBP50 in HEK293 resulted in a diffuse fluorescence signal throughout the cell that was not

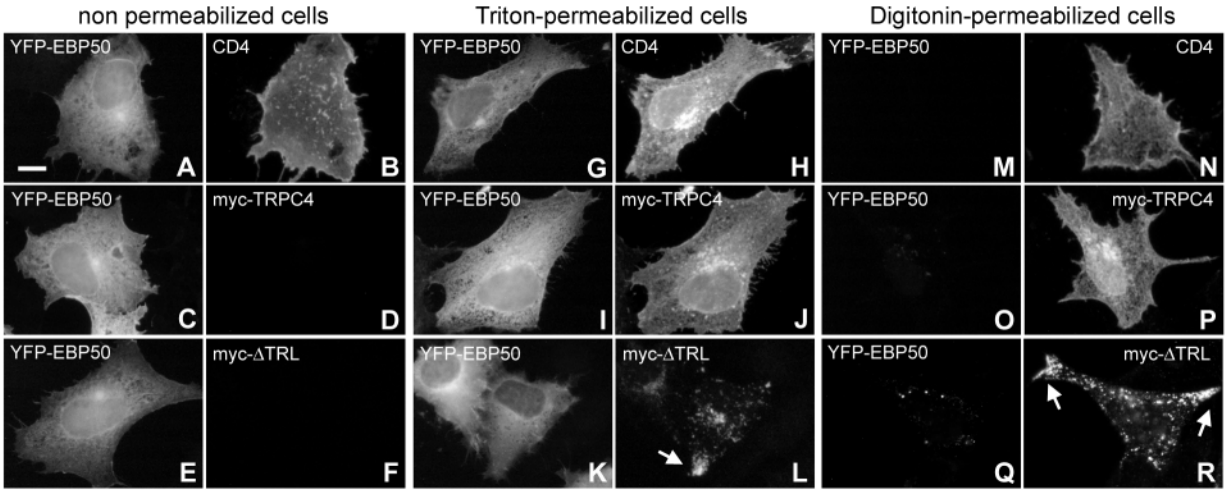

Fig. 4. Subcellular distribution of CD4, myc-TRPC4 and myc-ΔTRL in HEK293 cells co-expressing YFP-EBP50. (A-F) Non-permeabilized cells fixed with PFA. (G-L) Cells permeabilized with Triton X-100 after fixation. (M-R) Cells pre-extracted with digitonin before fixation. Upper panels: cells co-expressing YFP-EBP50 (A,G,M) and CD4 (B,H,N). Middle panels: cells co-expressing YFP-EBP50 (C,I,O) and myc-TRPC4 (D,J,P). Lower panels: cells co-expressing YFP-EBP50 (E,K,Q) and myc-ΔTRL (F,L,R). The arrows in L and R point to regions of myc-ΔTRL accumulation. To detect the transmembrane proteins, the transfected cells were probed with an anti-CD4 (upper panels) or an anti-myc (middle and lower panels) antibody and then stained with an Alexa 594-conjugated secondary antibody. Images were collected with a 100× oil immersion objective and filter sets for FITC (to detect YFP-EBP50) and Texas Red (to detect CD4 and the myc-tagged channels), using identical settings. Bar, 20 μm.

significantly influenced by co-expression of either CD4 (Fig. 4A,G), myc-TRPC4 (Fig. 4C,I) or myc-ΔTRL (Fig. 4E,K). In contrast to the transmembrane proteins (Fig. 4N,P,R), YFP-EBP50 was almost completely extracted by a pretreatment of the cells with a low concentration of digitonin prior to fixation (Fig. 4M,O,Q).

Deletion of the TRL motif at the C-terminus of TRPC4 decreases the fraction of channel associated with the plasma membrane

Whereas immunostaining clearly revealed differences in the subcellular distribution of the wild-type and truncated TRPC4 proteins, it did not allow quantification of channel expression on the cell surface. Thus, to compare the plasma membrane association of myc-TRPC4 and myc-ΔTRL in HEK293 cells (co-expressing YFP-EBP50), we performed cell surface biotinylation experiments. Equal amounts of transfected cells were treated with NHS-LC-biotin (at 4°C to prevent internalization of the biotin derivative) before being solubilized in Triton X-100. A portion of the resulting extract was retained as the total fraction. The remaining lysate was incubated with immobilized avidin to recover the biotinylated proteins. Serial dilutions of the total and surface fractions were resolved by SDS-PAGE, transferred to PVDF membrane and probed with the anti-myc antibody. Immunoreactive bands were visualized by ECL and quantified with a densitometer. Optical densities were then plotted against the respective amounts of total or biotinylated protein loaded. As shown in Fig. 5A, the intensity of the measured ECL signal was linear with respect to protein concentrations between 5 and 30 μg and volumes of avidin-precipitate between 10 and 40 μl. The slopes of the linear correlations were determined as described in Materials and Methods. The relative contents of myc-TRPC4 and myc-ΔTRL in the surface fraction and in the corresponding total extract, referred to as R_S and R_T, respectively, were then calculated by dividing the slope obtained from the myc-TRPC4-expressing cells by the slope derived from the myc-ΔTRL-expressing cells. Finally, R_S/R_T represents the relative content of myc-TRPC4 and myc-ΔTRL in the surface fraction corrected for any differences in the level of channel expression in the total extracts. Control experiments were performed to confirm that the avidin-bound myc-TRPC4 and myc-ΔTRL were derived only from the biotinylated pool of the surface molecules (see Materials and Methods and Fig. 5C).

As shown in Fig. 5B, expression on the cell surface was higher (~2.35-fold, $P<0.01$, one sample *t*-test) for myc-TRPC4 than for myc-ΔTRL in HEK293 cells co-expressing YFP-EBP50. Thus, deletion of the TRL motif not only changed the subcellular distribution of TRPC4 but also decreased its cell surface expression. These results may indicate that the anterograde trafficking of myc-ΔTRL to the plasma membrane is less efficient. They may also reflect a reduction in the residence time of the mutant at the cell surface. Indeed, EBP50 that interacts with the actin-binding protein of the ERM family, has been suggested to either prevent the internalization or facilitate the recycling to the plasma membrane of its target molecules. To determine whether the EBP50-ERM interaction influences the cell surface expression of TRPC4, a truncated form of EBP50 that lacks the ERM-binding domain was generated and fused to the YFP. The capability of the mutant (referred to as YFP-ΔERM) to interact with ezrin and myc-TRPC4 was analyzed first.

The YFP-EBP50 mutant lacking the ERM-binding site does not localize to the ezrin-enriched microvilli in JEG-3 cells but still associates with TRPC4 in HEK293 cells

As previously described, when expressed in JEG-3 cells, YFP-EBP50 (Fig. 6A) preferentially localized to the ezrin-enriched

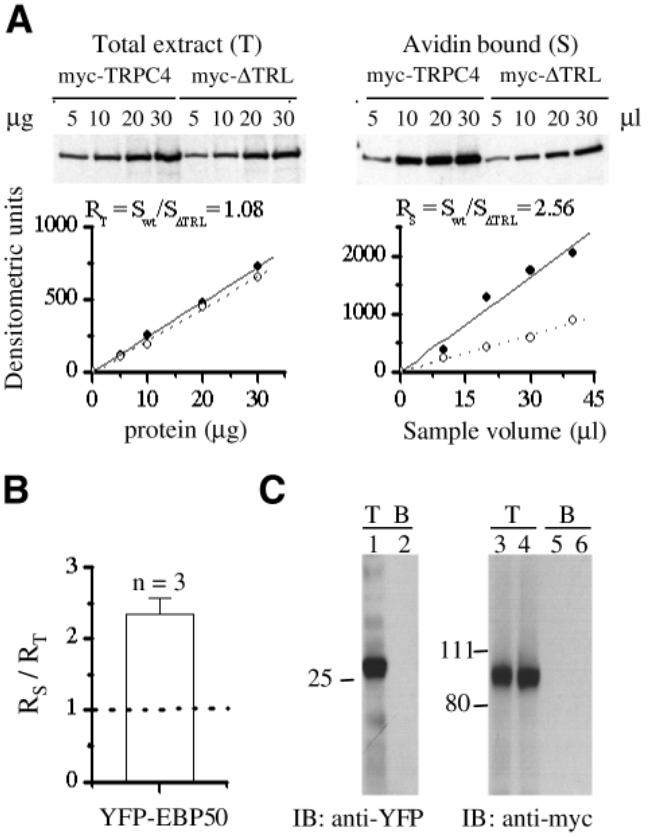

Fig. 5. Quantification of relative plasma membrane content of myc-TRPC4 and myc-ΔTRL in HEK293 cells by surface biotinylation. (A) myc-TRPC4 or myc-ΔTRL were transiently expressed in HEK293 cells together with YFP-EBP50. 48 hours after transfection, plasma membrane were biotinylated followed by cell lysis and incubation of lysates with avidin-agarose to recover biotinylated proteins. Total (left panel) and surface fraction (right panel) were separated by electrophoresis, electroblotted on PVDF and probed with an anti-myc antibody. Reactive bands were quantified with a densitometer. Optical densities of four dilutions of each sample were plotted against the amount of total (left panel) or biotinylated (right panel) proteins loaded. Lines indicate curves of best linear fit. The slopes of the correlations were determined. R_T (left panel) and R_S (right panel) were calculated by dividing S_{WT}, the slope obtained from the myc-TRPC4-expressing cells (filled circles, solid line) by $S_{\Delta TRL}$, the slope derived from the myc-ΔTRL-expressing cells (opened circles, dotted line). R_T and R_S represent the relative total and surface contents, respectively of myc-TRPC4 and myc-ΔTRL in transfected HEK293 cells. (B) The R_S/R_T ratio was determined from densitometry of three blot pairs similar to those presented in A and is shown as mean±s.e.m. (C) Degree of contamination with YFP (used as a marker of cytosolic proteins) or with non-biotinylated proteins. Monolayers were surface biotinylated (left panel) or exposed to the buffer alone (right panel) at 4°C for 30 minutes prior lysis. The cell extracts were incubated with avidin-agarose and the bound material, together with aliquots of the cell lysates, were separated by SDS-PAGE, transferred to PVDF and probed with either an anti-YFP (left panel) or an anti-myc (right panel) antibody. The absence of detectable avidin-bound YFP (lane 2), myc-TRPC4 (lane 5) or myc-ΔTRL (lane 6) suggests no contamination by biotinylated cytosolic proteins or intracellular myc-tagged channels. T, cell lysate (30 μg of protein); B, avidin-bound (40 μl of precipitate). Results shown are representative of three independent experiments.

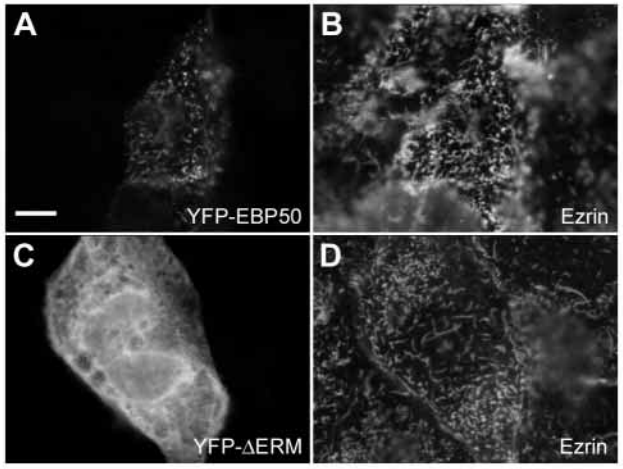

Fig. 6. Deletion of the ERM-binding domain modifies the subcellular distribution of YFP-EBP50 in human JEG-3 cells. JEG-3 cells transiently expressing YFP-EBP50 (A) or YFP-ΔERM (C) were fixed with PFA, permeabilized with triton, stained with an anti-ezrin antibody and then with an Alexa 594-conjugated secondary antibody. Images were acquired with a 100× oil immersion objective and filter sets for FITC (A,C) and Texas Red (B,D). Bar, 20 μm.

microvilli (Fig. 6A,B) of the apical surface. In contrast, YFP-ΔERM was found to be mainly cytosolic (Fig. 6C), the residual apical staining probably reflecting the association of the truncated mutant with endogenous EBP50 through PDZ-PDZ interactions (Fouassier et al., 2000). This redistribution was not due to an alteration of the morphology of the ezrin-rich structures in cells expressing YFP-ΔERM (Fig. 6D) and strongly suggests that the interaction with ezrin determines EBP50 localization in JEG-3 cells.

In HEK293 cells, YFP-EBP50 and YFP-ΔERM were expressed at similar levels and deletion of the 31 C-terminal amino acids of EBP50 did not impair its interaction with myc-TRPC4 (Fig. 7A). The subcellular distributions of the YFP-tagged proteins in myc-TRPC4- and myc-ΔTRL-expressing cells were compared upon cell fractionation. As shown in Fig. 7B (left panel), the partition of YFP-EBP50 between cytosolic and crude membrane fractions was not influenced by the co-expression of either myc-TRPC4 or myc-ΔTRL. In contrast, the amount of YFP-ΔERM associated with the crude membranes was found to be much higher in cells co-expressing myc-TRPC4 than in cells co-transfected with myc-ΔTRL (Fig. 7B, right panel). These results suggest that YFP-EBP50 and YFP-ΔERM primarily associate with membranes through their interaction with proteins of the ERM family and myc-TRPC4, respectively.

Disruption of the EBP50-ERM interaction decreases the fraction of TRPC4 associated with the plasma membrane

The effect of the disruption of the EBP50-ERM interaction on the surface expression of TRPC4 was then investigated. To compare the plasma membrane association of myc-TRPC4 in HEK293 cells co-expressing YFP-EBP50 or YFP-ΔERM, we performed cell surface biotinylation experiments. As shown in Fig. 8, the amount of myc-TRPC4 present at the cell surface

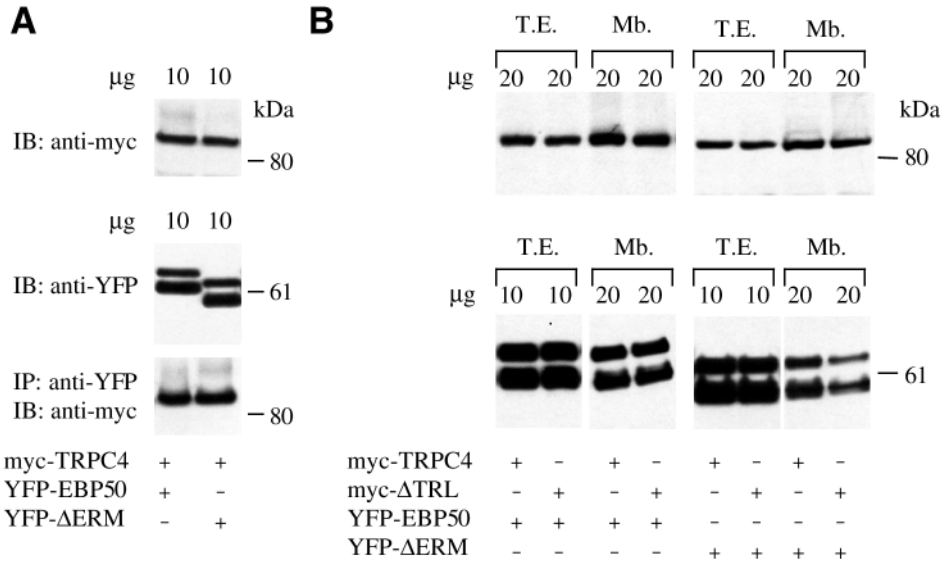

Fig. 7. (A) The YFP-EBP50 mutant lacking the ERM-binding site still associates with TRPC4 in HEK293 cells. Extracts of HEK293 cells expressing myc-TRPC4 together with YFP-EBP50 or YFP-ΔERM were incubated with an anti-YFP antibody and precipitated using Protein-G-coated agarose beads. Bound proteins were resolved on SDS-PAGE, transferred to PVDF and probed with an anti-myc antibody (lower panel). The upper and middle panels show the levels of expression of myc-TRPC4 and the YFP-tagged proteins, respectively, in the transfected cells. (Upper panel) ~15% input; (Lower panel) 40% precipitate. IB, immunoblot; IP, immunoprecipitation. (B) Deletion of the ERM-binding site decreases the membrane-associated fraction of YFP-EBP50. Western blots of total extracts (T.E.) and crude membrane fractions (Mb.) prepared from HEK293 cells expressing myc-TRPC4 or myc-ΔTRL together with either YFP-EBP50 or YFP-ΔERM. The amount of loaded proteins is indicated (µg). (Upper panels) Blots probed with an anti-myc antibody to detect myc-TRPC4 and myc-ΔTRL; (Lower panels) blots probed with an anti-YFP antibody to detect YFP-EBP50 and YFP-ΔERM. Molecular weights as revealed by prestained protein markers are indicated to the right (kDa). Results shown are representative of three independent experiments.

was significantly higher (~2.5-fold, $P<0.01$, one sample *t*-test) in cells co-transfected with YFP-EBP50 than in cells co-expressing the ΔERM mutant. Thus, disruption of the TRPC4-ERM interaction was found to have similar effects on the surface expression of TRPC4 as disruption of the TRPC4-EBP50 complex by mutation of the channel tail.

Disruption of the EBP50-ERM interaction prevents the translocation of TRPC4 from the cortical actin layer to the plasma membrane

The subcellular distributions of myc-TRPC4 and myc-ΔTRL in HEK293 cells overexpressing YFP-ΔERM were studied by indirect immunofluorescence microscopy. In about 60% of the transfected cells, the staining pattern of myc-TRPC4 was similar to that shown in Fig. 4J. However, in the remaining 40%, myc-TRPC4 and YFP-ΔERM were found to overlap in a perinuclear compartment, most probably representing the Golgi apparatus as well as in vesicles associated with filamentous structures that resembled cytoskeletal elements (Fig. 9A,B). The fact that this reticular phenotype was not detected in all the cells co-expressing myc-TRPC4 and YFP-ΔERM may indicate that the relative stoichiometry between the scaffold protein and its ligands is important for this process. YFP-ΔERM was expected to behave as a dominant interfering inhibitor of the TRPC4-ERM interaction. In some cells, the

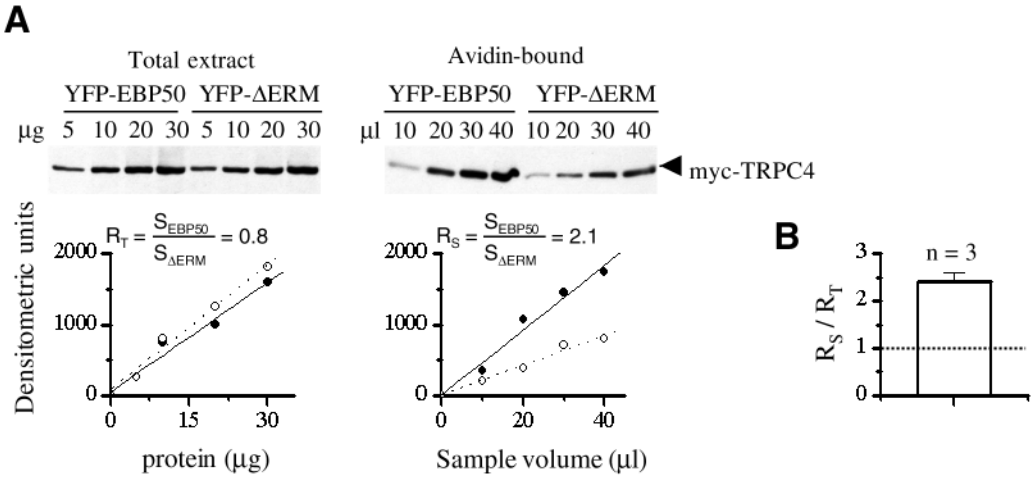

Fig. 8. Cell surface expression of myc-TRPC4 is altered by co-expression of the YFP-ΔERM mutant. Association of myc-TRPC4 with the plasma membrane in HEK293 cells expressing YFP-EBP50 or YFP-ΔERM was analyzed by cell surface biotinylation, as described in the legend to Fig. 5. (A) Representative western blots of total (left panel) and biotinylated proteins (right panel) extracted from HEK293 cells expressing myc-TRPC4 together with YFP-EBP50 or YFP-ΔERM. S_{EBP50} corresponds to the slope of the linear fit obtained from the YFP-EBP50-expressing cells (filled circles, solid line) and $S_{\Delta ERM}$ represents the slope of the linear fit derived from the YFP-ΔERM-expressing cells (open circles, dotted line). (B) Relative total (R_T) and surface (R_S) contents of myc-TRPC4, in YFP-EBP50- and YFP-ΔERM-expressing cells were calculated as described in the legend to Fig. 5. R_S/R_T was deduced from three blot pairs similar to those presented in A and is shown as mean±s.e.m.

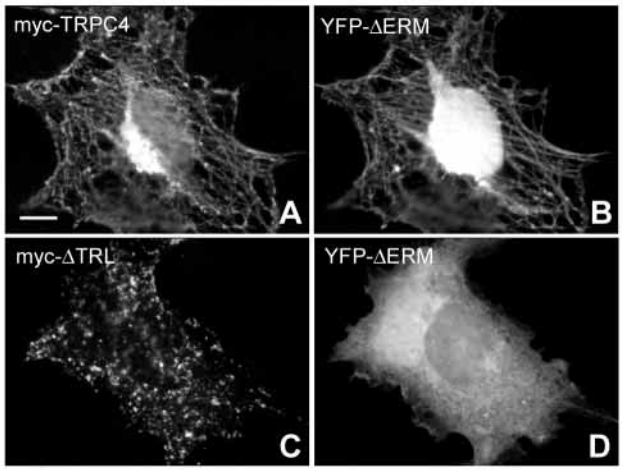

Fig. 9. Localization of myc-TRPC4 and myc-ΔTRL in HEK293 cells expressing YFP-ΔERM. HEK293 cells expressing YFP-ΔERM together with myc-TRPC4 (upper panels) or myc-ΔTRL (lower panels) were fixed with PFA, permeabilized with triton, stained with an anti-myc antibody and then with an Alexa 594-conjugated anti-mouse secondary antibody. Images were acquired with a 100× oil immersion objective and filter sets for Texas Red [to detect myc-TRPC4 (A) and myc-ΔTRL (C)] and for FITC [to detect YFP-ΔERM (B,D)]. Bar, 20 μm.

amount of mutant relative to endogenous EBP50 might, however, not have been sufficient to completely block the interaction with the endogenous proteins. By contrast, a large overexpression of YFP-ΔERM may favor the self-association of the scaffold protein rather than its interaction with other target molecules. Importantly, the reticular pattern was not seen in cells expressing YFP-ΔERM alone (data not shown) or together with myc-ΔTRL (Fig. 9C,D) suggesting that YFP-ΔERM and myc-TRPC4 need each other to associate with the filamentous structures.

To further characterize this phenotype, cells co-expressing YFP-ΔERM and myc-TRPC4 were stained with antibodies to various cytoskeletal proteins or with Texas-Red phalloidin. The reticular distribution of YFP-ΔERM (Fig. 10A) was not found to significantly overlap with the β tubulin (Fig. 10B) or vimentin (data not shown) immunostaining patterns. Interestingly, however, a significant proportion of the β tubulin was observed as discrete dot-like structures between the juxtanuclear filament mass and the cell surface (Fig. 10B) in cells co-expressing myc-TRPC4 and YFP-ΔERM, indicating that the microtubules were partially depolymerized. YFP-ΔERM (Fig. 10D) was found to mainly co-localize with the cortical actin layer beneath the plasma membrane and with actin cables within the cells (Fig. 10E), indicating that the YFP-ΔERM/myc-TRPC4 complex is able to bind to F-actin in an ERM-independent manner. The association of the myc-TRPC4-bearing vesicles with the cortical actin suggests that they were able to reach the submembranous compartment but not to fuse with the plasma membrane. Thus, we propose that the interaction between EBP50 and the proteins of the ERM family is required for the insertion of myc-TRPC4 in the plasma membrane.

Discussion

In this report, we have examined the influence of the PDZ-binding site formed by the last three C-terminal amino acids of TRPC4, on its subcellular distribution in transfected HEK293 cells. We have also analyzed the consequences of the interaction between EBP50 and the membrane-cytoskeletal adaptors of the ERM family for the surface expression of TRPC4.

A previous study has demonstrated that ^{35}S-labeled murine TRPC4 binds strongly to the first PDZ domain of NHERF (the rabbit ortholog of EBP50) and only weakly to the PDZ2 domain (Tang et al., 2000). Surprisingly, however, immobilized fusion proteins containing either the first or the second PDZ domain of EBP50 were found to precipitate myc-TRPC4 equally well from extracts of myc-TRPC4 expressing cells. The discrepancy between our data and the previously published results could indicate that, in our assay, the interaction between TRPC4 and the PDZ2 domain was not direct but mediated by another partner present in the cell lysate. Alternatively, the steady state binding equilibria might not have been established by the end of the pull-down assays in Tang's study since the GST-fusion proteins were incubated with in vitro translated TRPC4 for only 30 minutes. Indeed,

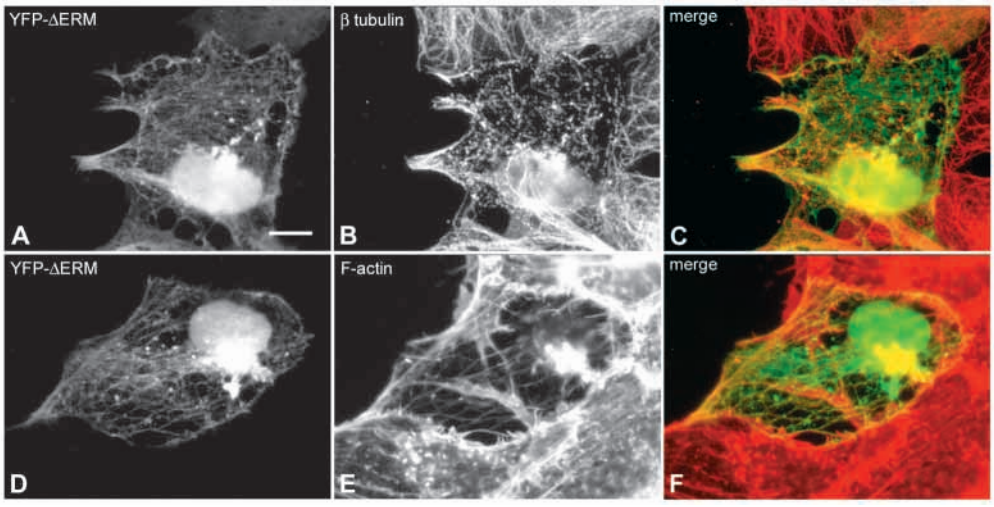

Fig. 10. Immunostaining of cytoskeletal elements in HEK293 cells co-expressing YFP-ΔERM and myc-TRPC4. HEK293 cells transiently expressing myc-TRPC4 together with YFP-ΔERM were fixed with PFA, permeabilized with triton, stained with either an anti-β-tubulin antibody and then with an Alexa 594-conjugated anti-mouse secondary antibody (A-C) or with phalloidin conjugated to Texas Red (D-F). Images were acquired with a 100× oil immersion objective and filter sets for FITC and Texas Red. YFP-ΔERM (A,D) and either β-tubulin (B) or F-actin (E) are overlaid in the panels on the right. Bar, 20 μm.

by performing surface plasmon resonance experiments, Raghuram et al. have recently shown that both PDZ domains of EBP50 strongly interact with the TRL motif present at the C-terminus of the cystic fibrosis transmembrane conductance regulator (CFTR) but that the PDZ2-CFTR complex is formed much slower than the PDZ1-CFTR interaction (Raghuram et al., 2001).

Deletion of the last three C-terminal amino acids (TRL) of TRPC4 was found to completely abolish the interaction with EBP50 and to alter both the localization and the surface expression of TRPC4 in HEK293 cells. Instead of being evenly distributed at the cell surface, the ΔTRL mutant accumulated into the cell outgrowths and its expression in the plasma membrane was 2.4 times lower than that of myc-TRPC4. Two non-exclusive hypotheses can be proposed to explain these results.

First, despite the fact that they do not show overt cell surface polarity, fibroblasts have apical and basolateral cognate routes for the delivery of newly synthesized proteins from the trans-Golgi network (TGN) to the plasma membrane (Musch et al., 1996; Yoshimori et al., 1996). Thus, the PDZ-binding site may be required for the efficient sorting of TRPC4 at the TGN level in HEK293 cells. In support of this hypothesis, deletion of the TRL motif present at the C-terminus of CFTR causes the redistribution of the truncation mutant from the apical to the basolateral membrane in airway epithelial cells (Moyer et al., 1999; Moyer et al., 2000) and epithelial basolateral proteins have been shown to accumulate into the cell outgrowths in nonpolarized cells (Grinstein et al., 1993; Peranen et al., 1996), such as myc-ΔTRL. Moreover, a PDZ-domain protein called CAL (CFTR-associated ligand), which mainly colocalizes with TGN markers in both epithelial and nonpolarized cells, has recently been identified (Cheng et al., 2001). CAL has been shown to bind to the C-terminus of CFTR and to modulate its surface expression.

Second, interaction of the C-terminus of TRPC4 with a PDZ-domain-containing protein may be required for the retention and the accumulation of TRPC4 at the cell surface. Indeed, through their association with the actin-binding protein of the ERM family, cortical scaffolds such as EBP50 or the related protein E3KARP may anchor TRPC4 to the cytoskeleton and prevent its internalization. In support of this hypothesis, CFTR molecules containing deletions that inhibit their interaction with EBP50 exhibit decreased expression and residence times in the plasma membrane of nonpolarized cells (Moyer et al., 2000). Alternatively, interaction of the C-terminus of TRPC4 with EBP50 may facilitate the recycling of internalized TRPC4 molecules to the plasma membrane, as recently shown for the β2-adrenergic receptor (Cao et al., 1999).

To analyze how the actin-linker function of EBP50 influences the cell surface expression of myc-TRPC4, an EBP50 mutant lacking the ERM-binding site was generated and co-expressed with myc-TRPC4 in HEK293 cells. In a large percentage of transfected cells, myc-TRPC4 and YFP-ΔERM were found to overlap in a perinuclear compartment, most probably representing the Golgi apparatus as well as in vesicles aligned along actin-filaments. YFP-ΔERM and myc-TRPC4 were found to need each other to associate with the cytoskeleton. We speculate that YFP-ΔERM first localizes to the Golgi apparatus through its interaction with the C-terminus of myc-TRPC4 and then mediates the anchoring of the post-Golgi vesicles containing myc-TRPC4 to the actin filaments. Two potential mechanisms can be proposed to explain how YFP-ΔERM may regulate the transfer of myc-TRPC4 from the TGN to the cortical actin network. First, YFP-ΔERM may be responsible for the sorting of TRPC4 in the TGN into specific vesicles, which are then transported along the actin microfilaments towards the cell surface. It has been shown that proteins that are sorted to the apical cognate route in fibroblasts become incorporated into lipid rafts in the TGN (Verkade and Simons, 1997; Zegers and Hoekstra, 1998) and that EBP50 interacts via its first PDZ domain with the broadly expressed raft-associated protein PAG (phosphoprotein associated with glycosphingolipid-enriched microdomains) (Brdickova et al., 2001). Thus, YFP-ΔERM may recruit TRPC4 into lipid rafts at the TGN through its interaction with a raft-resident protein such as PAG. Second, YFP-ΔERM may bind via one of its PDZ domains to an actin-based motor. In support of this hypothesis, INAD in *Drosophila* directly interacts with the unconventional myosin NINAC, which has been suggested to function as an actin-based motor (Bahler, 2000). Recent studies demonstrate that other multi-PDZ domains proteins including PDS-95 and LIN-10 also associate with post-Golgi vesicles and cytoskeleton components (El-Husseini et al., 2000; Setou et al., 2000). This may indicate a common role for PDZ-domain-containing proteins in transport of channel- or receptor-containing vesicles, ensuring reliability of transducisome assembly.

The association of myc-TRPC4 with the cortical actin layer suggests that TRPC4 can reach the submembranous compartment. However, the vesicles containing the cation channel seem to be trapped there and myc-TRPC4 is not delivered to the cell surface. We speculate that EBP50 binding to ezrin may allow the myc-TRPC4-bearing vesicles to leave the cortical actin and fuse with the plasma membrane. Interestingly, overexpression of CAL, which does not possess an ERM-binding site, was also found to decrease the cell surface expression of CFTR in COS-7 cells, in part by reducing the anterograde trafficking of CFTR to the plasma membrane (Cheng et al., 2001). The effects of CAL were reversed by overexpressing EBP50 (Cheng et al., 2001). Many findings support the hypothesis that the EBP50-ERM complex may play a role in the insertion of TRPC4 into the plasma membrane. First, at least two target molecules of the ERM proteins, namely the phosphatidylinositol (4,5)-biphosphate and the phosphatidylinositol 3-kinase (reviewed by Bretscher et al., 2000) have been shown to regulate fusion events. Second, EBP50 binds to EPI64 (EBP50-PDZ interactor of 64 kDa), a protein expressed in many cell types and containing a rab GTPase-activating protein (GAP) domain (Reczek and Bretscher, 2001). As a plasma membrane-associated rab-GAP, EPI64 would be expected to enhance the intrinsic rate of hydrolysis of GTP on the active rab on an incoming vesicle, perhaps providing a signal that it has reached the appropriate site. Finally, in parietal cells, the phosphorylation of subapically located ezrin, which allows its association with EBP50, has been correlated with the translocation and fusion of rab11a-containing vesicles with the apical surface (Urushidani and Forte, 1997). EBP50 binds only to activated ERM proteins and activation of the ERM proteins can be promoted by stimulation of surface receptors. Thus, PDZ proteins may be involved in determining the surface expression

of TRPC4 not only in basal conditions but also upon activation of the cells with specific stimuli.

In summary, we report that the last three C-terminal amino acids of TRPC4 comprise a PDZ-interacting domain, which controls the subcellular localization and surface expression of TRPC4 in HEK293 cells. Our data also suggest that TRPC4 insertion in the plasma membrane involves interaction with the ERM-bound scaffold EBP50. Because the EBP50 mutant that lacks the ERM-binding site was found to play a role in TRPC4 sorting at the TGN level and to be required for TRPC4 transport along actin microfilaments, we propose that another PDZ protein (such as CAL), which preferentially associates with the Golgi apparatus, may control the intracellular trafficking of TRPC4. In this view, the C-terminal domain of TRPC4 may sequentially interact with several PDZ proteins involved in targeting to the surface or insertion/retention in the plasma membrane, depending on their location within the cell.

The authors thank Veit Flockerzi, Barbara Niemeyer and Richard Zimmerman for helpful discussions and comments on the manuscript. This work was supported by grants from the Deutsche Forschungsgemeinschaft SFB 530 [Teilprojekt A3 (M.H.)], the Swiss National Science Foundation (3100-063696.00 and 31-55805.98) and the Novartis Stiftung.

References

Bahler, M. (2000). Are class III and class IX myosins motorized signaling molecules? *Biochim. Biophys. Acta* **1496**, 52-59.

Brdickova, N., Brdicka, T., Andera, L., Spicka, J., Angelisova, P., Milgram, S. L. and Horejsi, V. (2001). Interaction between two adapter proteins, PAG and EBP50: a possible link between membrane rafts and actin cytoskeleton. *FEBS Lett.* **507**, 133-136.

Bretscher, A., Chambers, D., Nguyen, R. and Reczek, D. (2000). ERM-Merlin and EBP50 protein families in plasma membrane organization and function. *Annu. Rev. Cell Dev. Biol.* **16**, 113-143.

Cao, T. T., Deacon, H. W., Reczek, D., Bretscher, A. and von Zastrow, M. (1999). A kinase-regulated PDZ-domain interaction controls endocytic sorting of the beta2-adrenergic receptor. *Nature* **401**, 286-290.

Cheng, S. H., Gregory, R. J., Marshall, J., Paul, S., Souza, D. W., White, G. A., O'Riordan, C. R. and Smith, A. E. (1990). Defective intracellular transport and processing of CFTR is the molecular basis of most cystic fibrosis. *Cell* **63**, 827-834.

Cheng, J., Moyer, B. D., Milewski, M., Loffing, J., Ikeda, M., Mickle, J. E., Cutting, G. G., Li, M., Stanton, B. A. and Guggino, W. B. (2001). A Golgi associated PDZ domain protein modulates cystic fibrosis transmembrane regulator plasma membrane expression. *J. Biol. Chem.* **277**, 3520-3529.

Chevesich, J., Kreuz, A. J. and Montell, C. (1997). Requirement for the PDZ domain protein, INAD, for localization of the TRP store-operated channel to a signaling complex. *Neuron* **18**, 95-105.

Clapham, D. E., Runnels, L. W. and Strubing, C. (2001). The TRP ion channel family. *Nat. Rev. Neurosci.* **2**, 387-396.

El-Husseini, A. E., Craven, S. E., Chetkovich, D. M., Firestein, B. L., Schnell, E., Aoki, C. and Bredt, D. S. (2000). Dual palmitoylation of PSD-95 mediates its vesiculotubular sorting, postsynaptic targeting, and ion channel clustering. *J. Cell Biol.* **148**, 159-172.

Fouassier, L., Yun, C. C., Fitz, J. G. and Doctor, R. B. (2000). Evidence for ezrin-radixin-moesin-binding phosphoprotein 50 (EBP50) self-association through PDZ-PDZ interactions. *J. Biol. Chem.* **275**, 25039-25045.

Grinstein, S., Woodside, M., Waddell, T., Downey, G., Orlowski, J., Pouyssegur, J., Wong, D. and Foskett, J. (1993). Focal localization of the NHE-1 isoform of the Na+/H+ antiport: assessment of effects on intracellular pH. *EMBO J.* **12**, 5209-5218.

Hall, R. A., Spurney, R. F., Premont, R. T., Rahman, N., Blitzer, J. T., Pitcher, J. A. and Lefkowitz, R. J. (1999). G protein-coupled receptor kinase 6A phosphorylates the Na+/H+ exchanger regulatory factor via a PDZ domain-mediated interaction. *J. Biol. Chem.* **274**, 24328-24334.

Kozak, M. (1991). An analysis of vertebrate mRNA sequences: intimations of translational control. *J. Cell Biol.* **115**, 887-903.

Li, H.-S. and Montell, C. (2000). TRP and the PDZ Protein, INAD, form the core complex required for retention of the signalplex in *Drosophila* photoreceptor cells. *J. Cell Biol.* **150**, 1411-1422.

Mery, L., Magnino, F., Schmidt, K., Krause, K. H. and Dufour, J. F. (2001). Alternative splice variants of hTRP4 differentially interact with the C-terminal portion of the inositol 1,4,5-trisphosphate receptors. *FEBS Lett.* **487**, 377-383.

Montell, C. (1999). Visual transduction in *Drosophila*. *Annu. Rev. Cell Dev. Biol.* **15**, 231-268.

Moyer, B., Denton, J., Karlson, K., Reynolds, D., Wang, S., Mickle, J., Milewski, M., Cutting, G., Guggino, W., Li, M. et al. (1999). A PDZ-interacting domain in CFTR is an apical membrane polarization signal. *J. Clin. Invest.* **104**, 1353-1361.

Moyer, B. D., Duhaime, M., Shaw, C., Denton, J., Reynolds, D., Karlson, K. H., Pfeiffer, J., Wang, S., Mickle, J. E., Milewski, M. et al. (2000). The PDZ-interacting domain of cystic fibrosis transmembrane conductance regulator is required for functional expression in the apical plasma membrane. *J. Biol. Chem.* **275**, 27069-27074.

Musch, A., Xu, H., Shields, D. and Rodriguez-Boulan, E. (1996). Transport of vesicular stomatitis virus G protein to the cell surface is signal mediated in polarized and nonpolarized cells. *J. Cell Biol.* **133**, 543-558.

Pasyk, E. A. and Foskett, J. K. (1997). Cystic fibrosis transmembrane conductance regulator-associated ATP and adenosine 3′-phosphate 5′-phosphosulfate channels in endoplasmic reticulum and plasma membranes. *J. Biol. Chem.* **272**, 7746-7751.

Peranen, J., Auvinen, P., Virta, H., Wepf, R. and Simons, K. (1996). Rab8 promotes polarized membrane transport through reorganization of actin and microtubules in fibroblasts. *J. Cell Biol.* **135**, 153-167.

Raghuram, V., Mak, D.-O. D. and Foskett, J. K. (2001). Regulation of cystic fibrosis transmembrane conductance regulator single-channel gating by bivalent PDZ-domain-mediated interaction. *Proc. Natl. Acad. Sci. USA* **98**, 1300-1305.

Reczek, D. and Bretscher, A. (2001). Identification of EPI64, a TBC/rabGAP domain-containing microvillar protein that binds to the first PDZ domain of EBP50 and E3KARP. *J. Cell Biol.* **153**, 191-206.

Reczek, D., Berryman, M. and Bretscher, A. (1997). Identification of EBP50: a pdz-containing phosphoprotein that associates with members of the ezrin-radixin-moesin family. *J. Cell Biol.* **139**, 169-179.

Rotin, D., Kanelis, V. and Schild, L. (2001). Trafficking and cell surface stability of EnaC. *Am. J. Physiol. Renal Physiol.* **281**, F391-F399.

Schaefer, M., Plant, T. D., Obukhov, A. G., Hofmann, T., Gudermann, T. and Schultz, G. (2000). Receptor-mediated regulation of the nonselective cation channels TRPC4 and TRPC5. *J. Biol. Chem.* **275**, 17517-17526.

Setou, M., Nakagawa, T., Seog, D. and Hirokawa, N. (2000). Kinesin superfamily motor protein KIF17 and mLin-10 in NMDA receptor-containing vesicle transport. *Science* **288**, 1796-1802.

Shieh, B. H. and Niemeyer, B. (1995). A novel protein encoded by the InaD gene regulates recovery of visual transduction in *Drosophila*. *Neuron* **14**, 201-210.

Songyang, Z., Fanning, A. S., Fu, C., Xu, J., Marfatia, S. M., Chishti, A. H., Crompton, A., Chan, A. C., Anderson, J. M. and Cantley, L. C. (1997). Recognition of unique carboxyl-terminal motifs by distinct PDZ domains. *Science* **275**, 73-77.

Tang, Y., Tang, J., Chen, Z., Trost, C., Flockerzi, V., Li, M., Ramesh, V. and Zhu, M. X. (2000). Association of mammalian TRPC4 and phospholipase C isozymes with a PDZ domain-containing protein, NHERF. *J. Biol. Chem.* **275**, 37559-37564.

Tsunoda, S., Sierralta, J., Sun, Y., Bodner, R., Suzuki, E., Becker, A., Socolich, M. and Zuker, C. S. (1997). A multivalent PDZ-domain protein assembles signaling complexes in a G-protein-coupled cascade. *Nature* **388**, 243-249.

Tsunoda, S., Sun, Y., Suzuki, E. and Zuker, C. (2001). Independent anchoring and assembly mechanisms of INAD signaling complexes in *Drosophila* photoreceptors. *J. Neurosci.* **21**, 150-158.

Urushidani, T. and Forte, J. (1997). Signal transduction and activation of acid secretion in the parietal cell. *J. Membr. Biol.* **159**, 99-111.

Verkade, P. and Simons, K. (1997). Robert Feulgen Lecture 1997. Lipid microdomains and membrane trafficking in mammalian cells. *Histochem. Cell Biol.* **108**, 211-220.

Wang, S., Yue, H., Derin, R., Guggino, W. and Li, M. (2000). Accessory protein facilitated CFTR-CFTR interaction, a molecular mechanism to potentiate the chloride channel activity. *Cell* **103**, 169-179.

Weinman, E. J., Steplock, D., Wang, Y. and Shenolikar, S. (1995). Characterization of a protein cofactor that mediates protein kinase A regulation of the renal brush border membrane Na(+)-H+ exchanger. *J. Clin. Invest.* **95**, 2143-2149.

Yoshimori, T., Keller, P., Roth, M. G. and Simons, K. (1996). Different biosynthetic transport routes to the plasma membrane in BHK and CHO cells. *J. Cell Biol.* **133**, 247-256.

Yun, C. H. C., Oh, S., Zizak, M., Steplock, D., Tsao, S., Tse, C.-M., Weinman, E. J. and Donowitz, M. (1997). cAMP-mediated inhibition of the epithelial brush border Na+/H+ exchanger, NHE3, requires an associated regulatory protein. *Proc. Natl. Acad. Sci. USA* **94**, 3010-3015.

Zegers, M. M. and Hoekstra, D. (1998). Mechanisms and functional features of polarized membrane traffic in epithelial and hepatic cells. *Biochem. J.* **336**, 257-269.

Zhou, Z., Gong, Q., Epstein, M. L. and January, C. T. (1998). HERG Channel Dysfunction in Human Long QT Syndrome: intracellular transport and functional defects. *J. Biol. Chem.* **273**, 21061-21066.